Supplementary Fig. 1

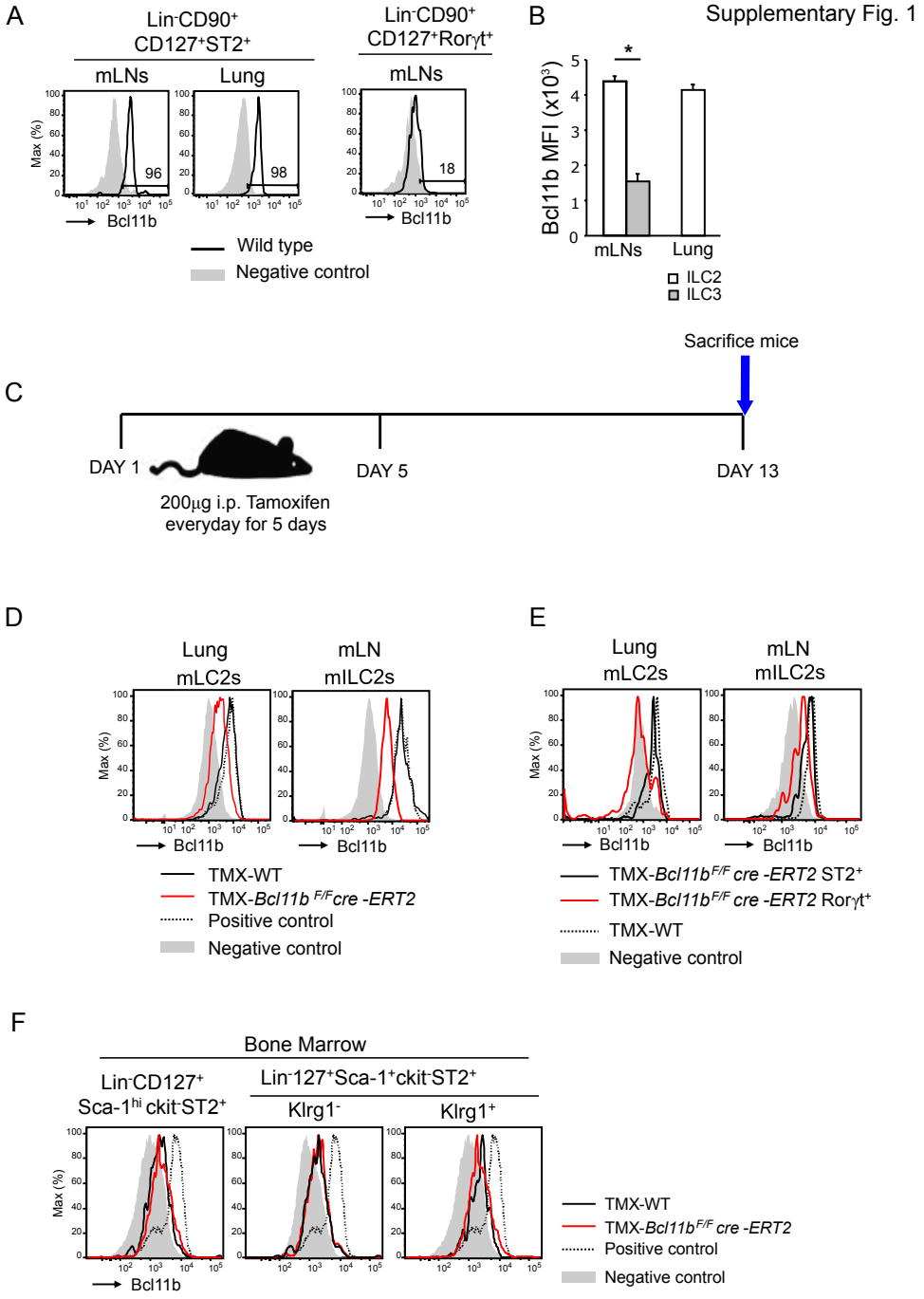

Figure S1 (related to Figure 1). Bcl11b is predominantly expressed in mature ILC2s in the periphery. A) Flow cytometry analysis of Bcl11b in ILC2s ($CD90^+Lin^-CD127^+T1ST2^+$) (black line) (left) and ILC3s ($CD90^+Lin^-CD127^+Ror\gamma t^+$) (black line) (right) in mesenteric lymph nodes (mLNs) and lung. Gray shaded area represents negative control. B) Mean fluorescence intensity (MFI) of Bcl11b in ILC2s and ILC3s in mLNs and lung. C) Experimental design of TMX-mediated *Bcl11b* deletion in *Bcl11b*$^{F/F}$*cre-ERT2* mice. D) Flow cytometry analysis of Bcl11b in ILC2s in the lung and mLNs of TMX-*Bcl11b*$^{F/F}$*cre-ERT2* (red) and -wild type control mice. Dashed line represents $CD3^+$ T cells, gray shaded area represents Lin^-CD90^- cells. E) Flow cytometry analysis of Bcl11b in $T1ST2^+$ (black) and $Ror\gamma t^+$ (red) ILC2s in the lung and mLN of TMX-*Bcl11b*$^{F/F}$*cre-ERT2* mice. Dashed line represents $CD3^+$ T cells and gray shaded area represents Lin^-CD90^- cells. F) Flow cytometry analysis of Bcl11b in the $Lin^-CD127^+Lin^-Sca\text{-}1^{hi}ckit^{lo}T1ST2^+$ (left panel), $CD127^+Lin^-Sca\text{-}1^{hi}ckit^{lo}T1ST2^+Klrg1^{lo}$ (middle panel), and $CD127^+Lin^-Sca\text{-}1^{hi}ckit^{lo}T1ST2^+Klrg1^+$ (right panel) populations in the bone marrow of TMX-*Bcl11b*$^{F/F}$*cre-ERT2* (red) and -wild type control (black) mice. Dashed line represents $CD3^+$ T cells and gray shaded area represents Lin^-CD127^- cells. Data (n=6) is representative of two independent experiments.

Supplementary Fig. 2

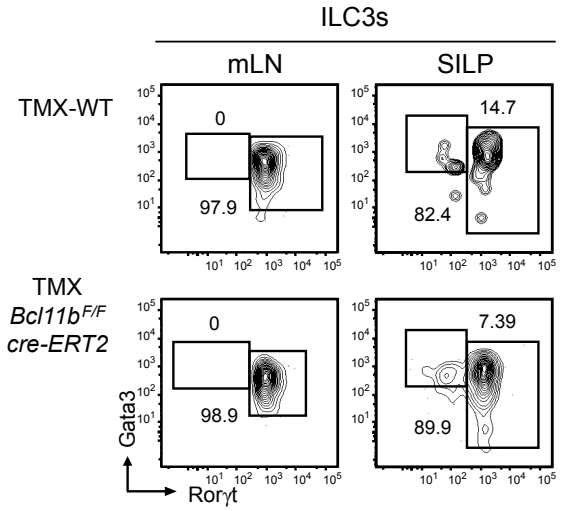

Figure S2 (related to Figure 1). ILC3s of TMX-*Bcl11b*$^{F/F}$*cre-ERT2-cre* mice do not exhibit altered expression of Gata3 and Rorγt. A) Gata3 vs Rorγt in the KLRG1^{lo} ILC population (ILC3s) from the mLNs and small intestine lamina propria (SILP) of TMX-*Bcl11b*$^{F/F}$*cre-ERT2* and -wild type control mice. Data (n=3) is representative of three independent experiments.

Supplementary Fig. 3

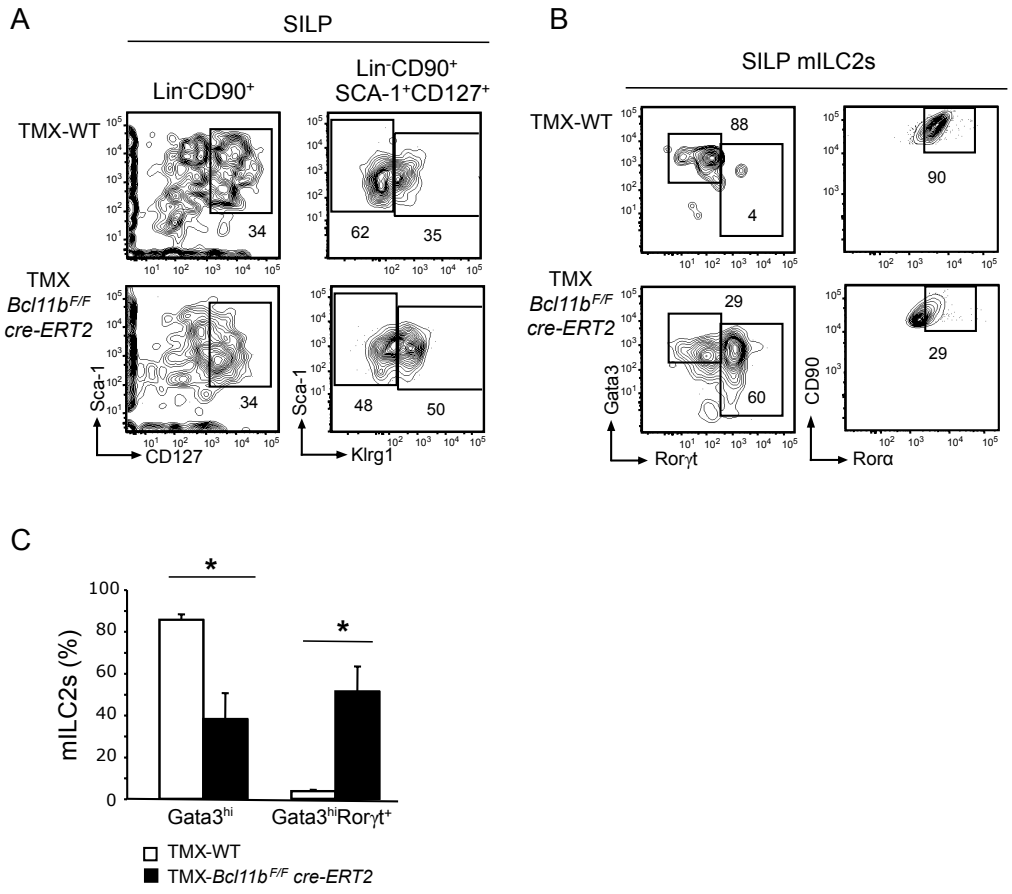

Figure S3 (related to Figure 1). *Bcl11b*$^{-/-}$ mature (m)ILC2s from the small intestine lamina propria (SILP) downregulate Gata3 and Rorα and upregulate the ILC3-specific transcription factor Rorγt. A) Flow cytometry analysis of Lin^{-}CD90^{+}Sca-1^{+}CD127^{+} ILCs

(left panel) and Klrg1^{hi} ILC2s (right panel) in the SILP of TMX-*Bcl11b*$^{F/F}$*cre-ERT2* and -wild type control mice. B) Gata3 vs. Rorγt (left panel) and CD90 vs. Rorα (right panel) in the mILC2s from the SILP of TMX-Bcl11b$^{F/F}$ ERT2-cre and TMX-wild type control mice. C) Average frequency of the Gata3^{hi}- and the Rorγt^{+}Gata3^{lo}-mILC2s in the SILP of TMX-*Bcl11b*$^{F/F}$*cre-ERT2* (black) and -wild type control (white) mice. Data (n=5), derived from three independent experiments, are presented as mean ± SEM. Significance was determined by Student's *t* test, * indicates p-value ≤ 0.05.

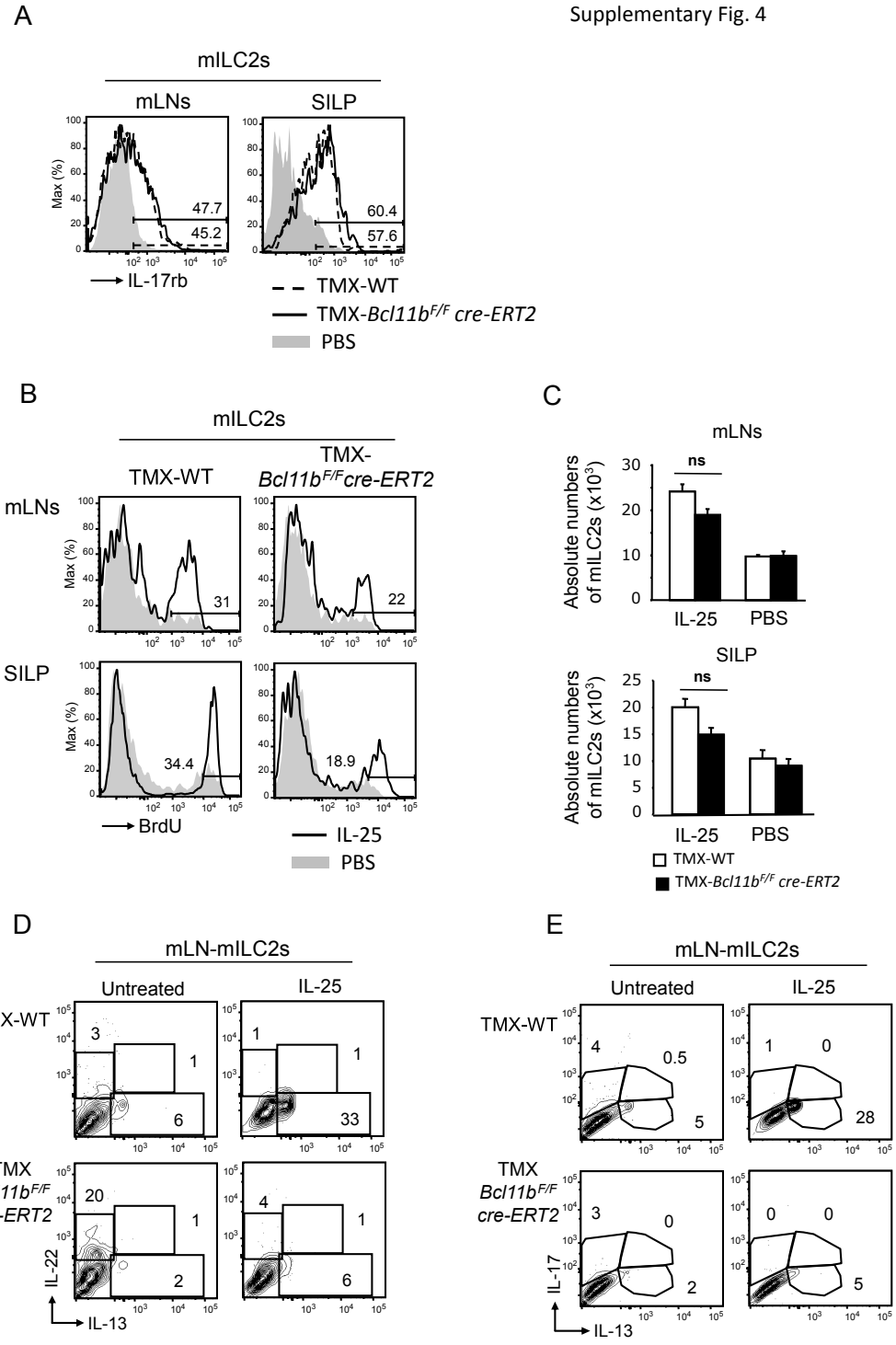
A
mILC2s
mLNs
SILP
Max (%)
47.7
45.2
60.4
57.6
IL-17rb
TMX-WT
TMX-Bcl11b F/F cre-ERT2
PBS
B
mILC2s
TMX-WT
TMX-Bcl11b F/F cre-ERT2
mLNs
SILP
Max (%)
31
22
34.4
18.9
BrdU
IL-25
PBS
C
mLNs
ns
Absolute numbers of mILC2s (x10 3)
IL-25
PBS
SILP
ns
Absolute numbers of mILC2s (x10 3)
IL-25
PBS
TMX-WT
TMX-Bcl11b F/F cre-ERT2
D
mLN-mILC2s
Untreated
IL-25
TMX-WT
3
1
6
1
1
33
TMX Bcl11b F/F cre-ERT2
20
1
2
4
1
6
IL-22
IL-13
E
mLN-mILC2s
Untreated
IL-25
TMX-WT
4
0.5
5
1
0
28
TMX Bcl11b F/F cre-ERT2
3
0
2
0
0
5
IL-17
IL-13

Figure S4 (related to Figure 3). *Bcl11b*$^{-/-}$ mILC2s from the mLNs and SILP express IL17rb and proliferate normally, but do not produce IL-13 in response to IL-25. A) Flow cytometry analysis of surface IL-17rb in mILC2s from the mLNs and SILP of TMX-*Bcl11b*$^{F/F}$*cre-ERT2* (black) and -wild type control (dashed) mice. Gray shaded area represents negative control. B) BrdU incorporation in mILC2s from mLNs and SILP of TMX-*Bcl11b*$^{F/F}$*cre-ERT2* and -wild type control mice treated with either IL-25 (black) or PBS (gray shaded area). C) Absolute numbers of mILC2s from the mLNs and SILP of the indicated groups of mice from the experiment described in (B). Data (n=5), derived from three independent experiments, are presented as mean ± SEM. Significance was determined by Student's *t* test, ns indicates p-value > 0.05. D-E) Flow cytometry analysis of intracellular IL-22 vs. IL-13 (D) and IL-17 vs. IL-13 (E) in mILC2s from the mLNs of IL-25 or PBS treated TMX-*Bcl11b*$^{F/F}$*cre-ERT2* and -wild type control mice. Data (n=4) derived from three independent experiments.

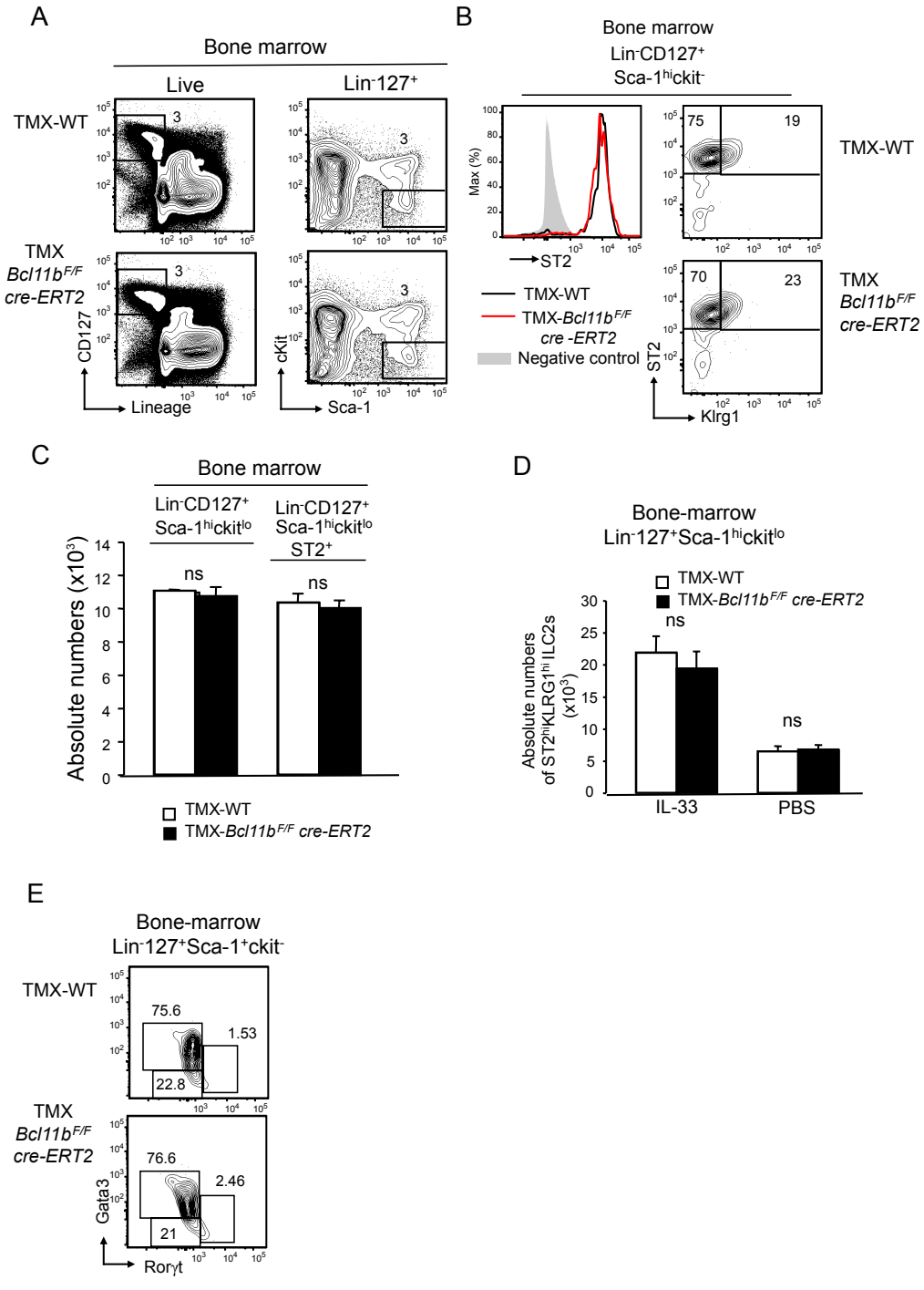
A
Bone marrow
Live
Lin-127+
TMX-WT
TMX Bcl11bF/F cre-ERT2
CD127
Lineage
cKit
Sca-1
B
Bone marrow
Lin-CD127+
Sca-1hickit-
Max (%)
ST2
TMX-WT
TMX-Bcl11bF/F cre -ERT2
Negative control
75
19
70
23
ST2
Klrg1
C
Bone marrow
Lin-CD127+ Sca-1hickitlo
Lin-CD127+ Sca-1hickitlo ST2+
Absolute numbers (x10³)
ns
TMX-WT
TMX-Bcl11bF/F cre-ERT2
D
Bone-marrow
Lin-127+Sca-1hickitlo
TMX-WT
TMX-Bcl11bF/F cre-ERT2
Absolute numbers of ST2hiKLRG1hi ILC2s (x10³)
IL-33
PBS
E
Bone-marrow
Lin-127+Sca-1+ckit-
TMX-WT
75.6
1.53
22.8
TMX Bcl11bF/F cre-ERT2
76.6
2.46
21
Gata3
Rorγt

Figure S5 (related to Figure 1). Bcl11b does not regulate identity of the bone marrow ILC2s. A) Flow cytometry analysis of the Lin^- $CD127^+$ (left panel), and $Lin^-Sca\text{-}1^{hi}ckit^{lo}$ $CD127^+$ (right panel) populations in the bone marrow of TMX-*Bcl11b*$^{F/F}$*cre-ERT2* and -wild type control mice. B) FACS analysis of ST2 (left panel) and ST2 vs. Klrg1 (right panel) in the $Lin^-Sca\text{-}1^{hi}ckit^{lo}$ $CD127^+$ population from the bone marrow of the indicated mice. Gray shaded area represents negative control. C) Absolute numbers of $Lin^-Sca\text{-}1^{hi}ckit^{lo}$ $CD127^+$ precursors and $Lin^-CD127^+Lin^-Sca\text{-}1^{hi}ckit^{lo}ST2^+$ precursors in the bone marrow of TMX-*Bcl11b*$^{F/F}$*cre-ERT2* (black) and -wild type control (white) mice. Data (n=8), derived from three independent experiments, are presented as mean ± SEM. Significance was determined by Student's *t* test, ns means non-significant, $p > 0.05$. D) Average frequency $ST2^+$ $Klrg1^{hi}$ cells in the $Lin^-Sca\text{-}1^{hi}ckit^{lo}$ $CD127^+$ population in IL-33- or PBS-treated TMX-*Bcl11b*$^{F/F}$*cre-ERT2* (black) and -wild type control (white) mice. E) Gata3 vs. Rorγt in the $Lin^-CD127^+Lin^-Sca\text{-}1^{hi}ckit^{lo}$ precursors from the bone marrow of TMX-*Bcl11b*$^{F/F}$*cre-ERT2* and TMX-wild type control mice. Data (n=6) is representative of three independent experiments.

Supplementary Fig. 6

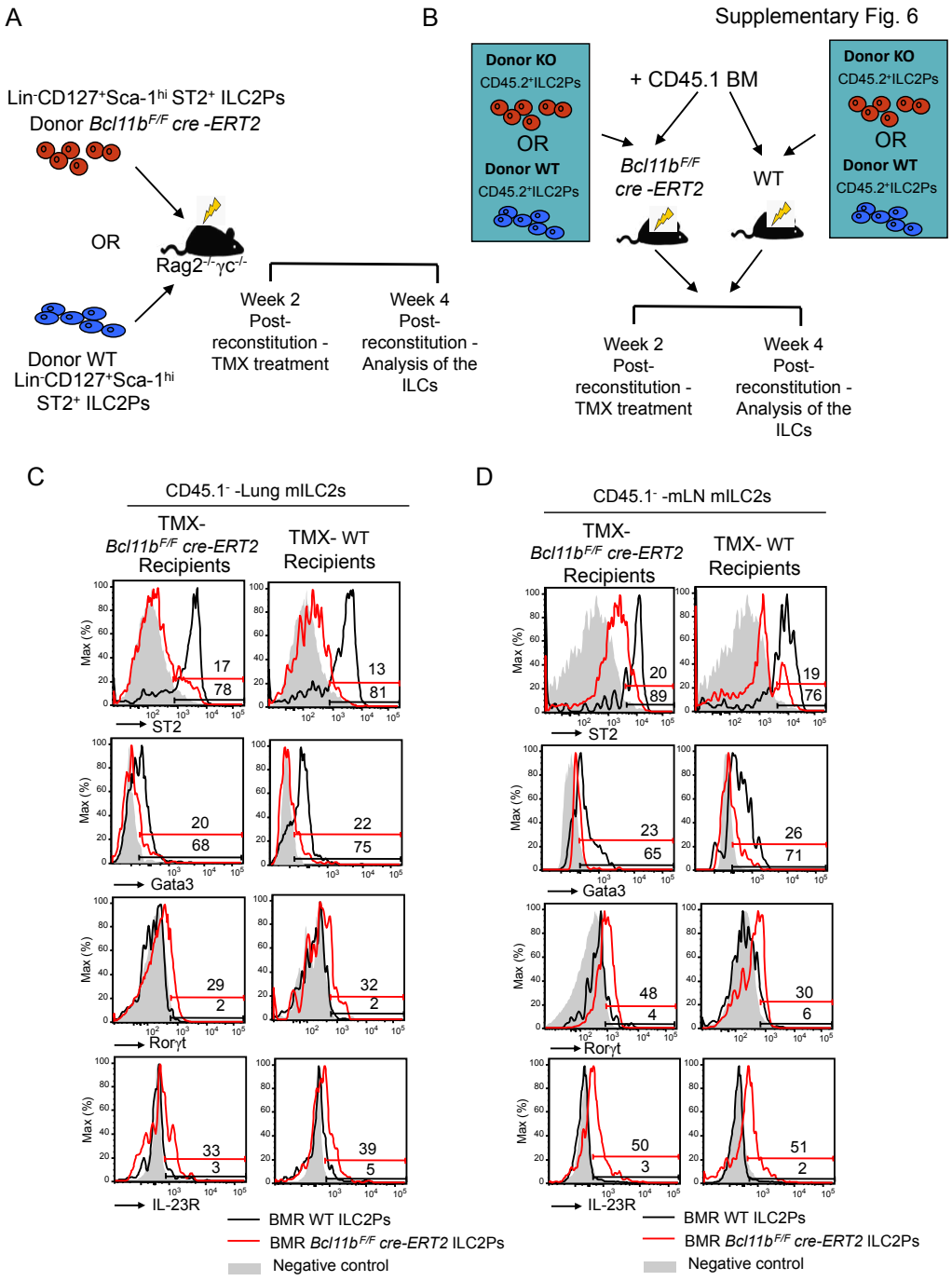

Figure S6 (related to Figure 2). Bcl11b-mediated regulation of mILC2s identity is not dependent on non-hematopoietic compartment. (A and B) Experimental design for bone marrow reconstitution experiments. A) Sorted ILC2 precursors ($Lin^{-}Sca\text{-}1^{hi}CD127^{+}T1ST2^{+}$) from the bone marrow of *Bcl11b*$^{F/F}$*cre-ERT2* and wild type control mice were injected into sub-lethally irradiated $Rag2^{-/-}\gamma c^{-/-}$ recipient mice. Two weeks post-reconstitution, recipients were treated with TMX, followed by evaluation of ILC2 populations in the lung and SILP at four weeks post-reconstitution. B) Sorted ILC2 precursors ($CD127^{+}Lin^{-}Sca\text{-}1^{hi}T1ST2^{+}$) from the bone marrow of *Bcl11b*$^{F/F}$*cre-ERT2* or wild type control mice were injected, along with the bone marrow from CD45.1 mice, into lethally irradiated *Bcl11b*$^{F/F}$*cre-ERT2* and wild type control recipients. Two weeks post-reconstitution, recipients were treated with TMX, followed by evaluation of ILC2 populations in the lung and SILP at four weeks post-reconstitution. C-D) ST2, Gata3, Rorγt and IL-23R in the 45.1^{-} lung (C) and mLNs (D) mILC2s of TMX-*Bcl11b*$^{F/F}$*cre-ERT2* mice or wild type mice reconstituted with bone marrow ILC2Ps from untreated *Bcl11b*$^{F/F}$*cre-ERT2* (red) or wild type (black) mice. Gray shaded area represents negative control. Data (n=5) is representative of two independent experiments.

A

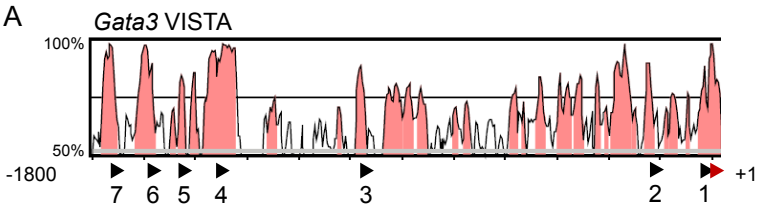

B

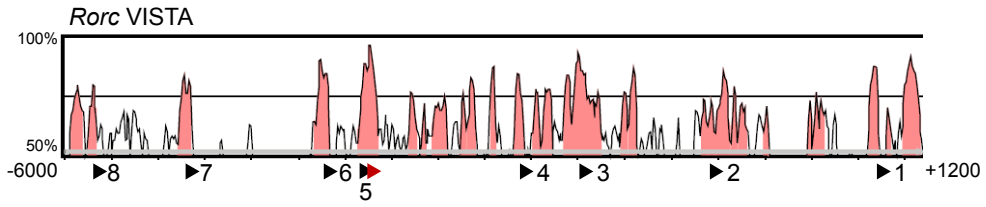

C

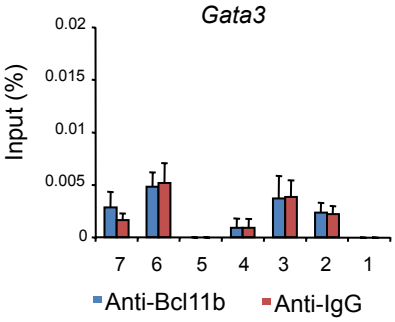

D

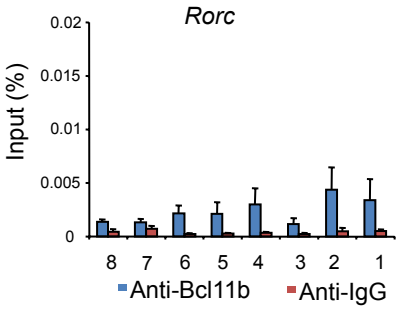

E

	Forward 5'-3'	Reverse 5'-3'
Gfi1 region 1	ATACCCCCTTCCTGTCACCT	ACTTCCTGAGCGTTAGAGGC
Gfi1 region 2	CCCGAGGCGCAGGTTTC	TTTGCGCAAGGGGTCAGGA
Gfi1 region 3	TTCAGCTTCGTTGGGCGTAT	ATCCTGTCGACTGTTTGGGC
Ahr region 1	CACTACGTCCTGCGTCATCA	CGCCCCACCTGCTCG
Ahr region 2	ACCTATGCAACTACCTGATGAACT	CTAGTGATAACAGACAGGCTCCA
Ahr region 3	CCATCAACTTCCCCATGACTGA	GCCTAACATGCTGTGCGTCTA
Ahr region 4	TGTCAGCACTATACAAGCCTCC	TCACTGGCAGAAAGAAAGCCA
Ahr region 5	GACTGAAGGCCAAAACATCGTA	AAAAGCCATATGCACTCTCCC

F

	Forward 5'-3'	Reverse 5'-3'
Gata3 region 1	CCTGGAGCGGGTTTGGGTTG	TCTAGTGTCATCCGCGCCGA
Gata3 region 2	CCAGCTTTTTATGCATCGCGTTGT	CAGAACGAACAGCGTCAGCTGT
Gata3 region 3	GACTTCATGGTTCAGCCACGGAC	TCAGGGTCCATTTGTTTTGGCAGG
Gata3 region 4	GGTAAAGCACGGGCAGGCAA	GTGGAAAGCGATGGCCAGCA
Gata3 region 5	GGGAGGGGTTCTGGAACTCCG	CACCCTTTAAGCTCCCTGTGCG
Gata3 region 6	GAACCGGCCAGTAGGCTCCA	CAGCCTCAGCCATGGAAGTGC
Gata3 region 7	CGCAGCGGTAACGCAGACAT	GGACCTGGAGCCGGGCTAAA
Rorc region 1	AGCTTTGCTGTGGAAGATGTTTC	GAAGGGCTGGTAGGGAAGTCA
Rorc region 2	GCTTCTTCCTCCTGGTGATTCA	GAGGAAATAAAAGAACGCAAAGAAA
Rorc region 3	ACCTGTGTGGAGCAGAGCTT	TGCCCCCATTCACTTACTTC
Rorc region 4	TGATCAGCCTCCTGTGCACTA	TGCGTCATTCTGACTCGCTTT
Rorc region 5	CTTTCACCTGTTTTTCCTCAAGACT	AGGAGTGGCTGGCAGAGTGT
Rorc region 6	GCTCCTGCCCTGCTGTTTAC	TTAGCTGTGCCTGGCTTTCC
Rorc region 7	CACCACCCACCTCCAGGTT	CGTGCCCAGTCCTCTTATCAG
Rorc region 8	TGCTCCAGTTGTCCACCAGAT	CCATTGATCAGGTTGCTGTCA

Figure S7 (related to Figure 6). Bcl11b does not associate with *Gata3* proximal promoter and conserved noncoding regions (CNSs) at the *Rorc* locus. A-B) Vista alignment of mouse and human *Gata3* promoter (A) and *Rorc* -6000bp-+1200bp (B) showing conserved regions (pink peaks). Black triangles indicate the regions amplified by qPCR following ChIP. Red triangle represents TSS. The 8 pairs of *Rorc* primers were designed based on the information provided by (Malhotra et al., 2013; Ruan et al., 2011; Tanaka et al., 2014). C-D) Chromatin immunoprecipitation (ChIP) by anti-Bcl11b antibodies (Blue) or IgG (pink) of cross-linked nuclear extracts from sorted Lin^- $CD90^+Klrg1^+$ ILC2s expanded *in vitro* as described in Material and methods. ChIP-ed DNA was amplified by qPCR with primers for the indicated conserved regions (sequence provided in E and F). Data (n=6), derived from representative of two independent experiments, are presented as mean ± SEM. Significance determined by Student's *t* test. E-F) Sequence of primers used in ChIP assays in experiments for Figure 6 (A and C) and Figure S7 (C and D). Primers for Gfi1 were designed based (Yucel et al., 2004).

Supplementary Material and Methods

Cytokine-induced BrdU incorporation. Mice were administered with either 500ng IL-23 or IL-33 via i.p. injection and intranasally on day 0, and on days 1 and 3, respectively. For BrdU incorporation, 1mg/ml BrdU was administered by i.p. injection on days 2 and 3. On day 4 mice were sacrificed and evaluated for BrdU incorporation in the mILC2s from lung, mLNs and SILP. BrdU staining followed surface staining and was conducted using fixation and permeabilization buffers (ebioscience) with Protocol B.

ILC2 maturation. Mice were administered IL-33 via i.p. injection as described above. On day 4 mice were sacrificed and bone marrow ILC2Ps were evaluated for $Lin^{-}CD127^{+}Sca\text{-}1^{hi}ckit^{lo}ST2^{hi}Klrg1^{hi}$ by flow cytometry.

In vivo stimulation of cytokine production. Mice were administered with either 500ng of IL-23, IL-25 or IL-33 via i.p. injection on days 0-3. On day 4 mice were sacrificed and ILCs were evaluated for cytokine production by intracellular cyokine staining as described below.

Bone Marrow Chimeras. 5,000 sorted $Lin^{-}CD127^{+}Sca\text{-}1^{hi}ST2^{+}$ ILC2Ps from BM were intravenously injected into sub-lethally irradiated (500 rads) $Rag2^{-/-}\gamma c^{-/-}$ recipient mice (Figure S6A). Alternatively, 5,000 sorted $Lin^{-}CD127^{+}Sca\text{-}1^{hi}ST2^{+}$ ILC2Ps from BM were intravenously injected into lethally irradiated $Bcl11b^{F/F}$ Cre-ERT2 (CD45.2) and wild type mice (CD45.2). For lethally irradiated recipients, $1X10^{6}$ CD45.1 BM cells were also transferred. Two weeks post-reconstitution, recipient mice were treated with tamoxifen, and ILC2s from the lung, mLNs and SILP were analyzed 4 weeks post-transfer.

Intracellular cytokine staining: Cells were stimulated for four hours with 50 ng/ml PMA and 500 ng/ml Ionomycin in CM at 37°C, with 10 μg/ml Brefeldin A. Cells were stained for surface markers, followed by fixation in 4% paraformaldehyde. Permeabilization of cells with 0.05% saponin buffer was performed before intracellular staining.

Flow Cytometry: Flow cytometry analyses were performed on a FacsCalibur upgraded to three lasers and eight colors and digital acquisition (Cytek) using FlowJo software. Data was analyzed using FlowJo software (Tree Star Inc.).

Antibodies: Cells were surface stained with following antibodies: anti- anti-CD3e (145-2C11), anti-CD19 (eBio1D3), anti-CD5 (53-7.3), anti-TCRβ (H57-597), anti-NK1.1 (PK136), anti-CD11b (M1/70), anti-CD11c (N418), anti-CD90.2 (30-H12), anti-CD127 (A7R34), anti-KLRG1 (2F1), anti-IL-13 (ebio13A), anti-IL-5 (TRFK5), anti-IL17 (ebio17B7), anti-IL22 (IL22JOP), anti-Ly6C (HK1.4) anti-α4β7 (DATK32), anti-CD117 (2B8), anti-Rorγt (B2D) (from ebioscience); GATA3 (L50-823), anti-IL23R (O78-1208), anti-Siglec F (E50-2440) (from BD biosciences); anti-ST2 (DIH9), anti-IL17rb (9B10), anti-Sca-1 (D7), anti-Ly6G (1A8), anti-GFP (FM264G) (from biolegend); anti-ST2 (DJ8) (rom MDBioproducts); and anti-RORα (from Bioss).

Chromatin immunoprecipitation. ILC2s ($Lin^-CD90^+Klrg1^+$) were sorted from mLNS and SILP of wild type mice, then expanded *in vitro* with 10 ng/ml IL-2, IL-7, and IL-33 for 10 days. ILC2s were fixed with 1% formaldehyde for 4 minutes at room temperature followed by the addition of glycine to the stop reaction. Fixed cells were then washed with cold PBS, and resuspended in lysis buffer. Chromatin was sheared in a chemical reaction using Micrococcal Nuclease for 20 minutes at 37^{o}C, then the nuclear membrane was broken by sonication for 20 seconds at setting 6 using Microson^{TM} Ultrasonic Cell Disruptor XL (Misonix). Chromation immunoprecipitation was performed by adding 10 µL of 1 mg/mL rabbit α-Bcl11b antibody (affinity purified, BL1801, A300-385A, Bethyl) to the chromatin preparation, and incubated overnight at 4^{o}C with rotation. The antibody-chromatin complex was isolated with ChIP Grade Protein G Magnetic Beads (Cell signaling Technology), washed, eluted and reverse-crosslinked. DNA was purified and quantification of DNA was performed by real-time quantitative PCR using the primers

listed in Figure S7E-F.

References

Malhotra, N., Narayan, K., Cho, O.H., Sylvia, K.E., Yin, C., Melichar, H., Rashighi, M., Lefebvre, V., Harris, J.E., Berg, L.J., and Kang, J. (2013). A network of high-mobility group box transcription factors programs innate interleukin-17 production. Immunity *38*, 681-693.

Ruan, Q., Kameswaran, V., Zhang, Y., Zheng, S., Sun, J., Wang, J., DeVirgiliis, J., Liou, H.C., Beg, A.A., and Chen, Y.H. (2011). The Th17 immune response is controlled by the Rel-RORgamma-RORgamma T transcriptional axis. J Exp Med *208*, 2321-2333.

Tanaka, S., Suto, A., Iwamoto, T., Kashiwakuma, D., Kagami, S., Suzuki, K., Takatori, H., Tamachi, T., Hirose, K., Onodera, A.*, et al.* (2014). Sox5 and c-Maf cooperatively induce Th17 cell differentiation via RORgammat induction as downstream targets of Stat3. J Exp Med *211*, 1857-1874.

Yucel, R., Kosan, C., Heyd, F., and Moroy, T. (2004). Gfi1:green fluorescent protein knock-in mutant reveals differential expression and autoregulation of the growth factor independence 1 (Gfi1) gene during lymphocyte development. J Biol Chem *279*, 40906-40917.